


Nematic superconductivity in topological insulators induced by hexagonal warpingR. S. Akzyanov,^{1,2,3} D. A. Khokhlov ^{1,2,4} and A. L. Rakhmanov^{1,3,2}¹*Dukhov Research Institute of Automatics, Moscow 127055, Russia*²*Moscow Institute of Physics and Technology, Dolgoprudny, Moscow Region 141700, Russia*³*Institute for Theoretical and Applied Electrodynamics, Russian Academy of Sciences, Moscow 125412, Russia*⁴*National Research University Higher School of Economics, Moscow 101000, Russia* (Received 16 March 2020; revised 16 June 2020; accepted 26 August 2020; published 14 September 2020)

We study the superconducting properties of the bulk states of a doped topological insulator. We obtain that hexagonal warping stabilizes the nematic spin-triplet superconducting phase with E_u pairing and the direction of the nematic order parameter which opens the full gap is the ground state. This order parameter exhibits non-BCS behavior. The ratio of the order parameter to the critical temperature of $\Delta(0)/T_c$ differs from the BCS ratio. It depends on the chemical potential and the value of the hexagonal warping. We discuss the relevance of the obtained results for the explanation of the experimental observations.

DOI: [10.1103/PhysRevB.102.094511](https://doi.org/10.1103/PhysRevB.102.094511)**I. INTRODUCTION**

The nontrivial band structure of topological insulators brings about fascinating phenomena such as robust gapless surface states and “topological” electromagnetic responses [1]. Proximity-induced superconductivity in topological insulators attracts attention due to the possible existence of Majorana fermions [2]. Upon doping, the topological insulator becomes a bulk superconductor. Along with s -wave pairing with A_{1g} symmetry, topologically nontrivial pairings with A_{1u} , A_{2u} , and E_u symmetries become possible [3]. The E_u symmetry corresponds to the vector nematic order parameter with triplet pairing that breaks rotational symmetry. Such a nematic phase supports Majorana fermions [4], surface Andreev bound states [5], vestigial order [6], and unconventional Higgs modes [7]. Recently, it was shown that the nematic phase may compete with a chiral superconducting phase that breaks time-reversal symmetry [8,9].

There is a lot of experimental evidence for nematic superconductivity with E_u pairing in doped topological insulators [10]. In particular, the data on the Knight shift support the spin-triplet nature of the superconducting order parameter in Cu-doped Bi_2Se_3 [11]. The breaking of rotational symmetry was observed in heat [12], magnetotransport [13], and scanning tunneling microscopy (STM) measurements [14,15]. Recently, it has been demonstrated that the strain dictates the direction of the anisotropy of the second critical field in $\text{Sr}_x\text{Bi}_2\text{Se}_3$ [16], which unambiguously confirms that the ground state in this topological insulator is nematic superconductivity with E_u symmetry [17]. Contact measurements show that the ratio of the superconducting gap to the critical temperature in a doped topological insulator differs from that in BCS s -wave superconductors [15,18,19].

At first sight, the origin of nematic superconductivity in doped topological insulators is a mystery. In their seminal work [3], Fu and Berg show that the triplet superconducting order parameter with an A_{1u} representation is

always favorable in comparison to the nematic order with an E_u representation and competes with the usual s -wave pairing in topological insulators. Later, it was argued that electron-electron repulsion in $\text{Cu}_x\text{Bi}_2\text{Se}_3$ favors A_{1u} order [20,21], while in Refs. [4,22], the authors suggested that a strong Coulomb repulsion between electrons can stabilize nematic superconductivity. However, this mechanism is doubtful in the case of topological insulators since the huge dielectric constant in this system implies a weak electron-electron Coulomb interaction. That was confirmed by analysis of the angle-resolved photoemission spectroscopy (ARPES) data [23].

In this paper, we calculate the phase diagram of a doped topological insulator with attractive coupling between charge carriers. Following the approach of Ref. [3], we calculate the superconducting susceptibility of the bulk states to determine the critical temperature of the superconducting phases. Then, we specify our results by calculating the free energy. In Ref. [3], the low-energy expansion of the Hamiltonian has been used by taking into account only linear terms to elucidate the main features of the problem. In our calculations, we included the term which is responsible for the hexagonal warping of the Fermi surface. This term is proportional to the third power of the momentum and arises due to the crystal symmetry of the topological insulators [24,25]. Hexagonal warping affects significantly the charge and spin transport in topological insulators [26,27]. It also is of importance for the characteristics of nematic superconductivity: The presence of hexagonal warping gives rise to a full superconducting gap in the spectrum [17]. We found that hexagonal warping stabilizes the superconducting phase with a nematic E_u order. If hexagonal warping is significant, the nematic phase becomes a ground state. This result can explain the observations of nematic E_u superconductivity in experiments with doped topological insulators. We calculate the ratio of the superconducting order parameter at zero temperature to the critical temperature and obtain that, in contrast to the

TABLE I. Possible superconducting pairings taken from Ref. [3].

	$\hat{\Delta}_1$	$\hat{\Delta}_2$	$\hat{\Delta}_3$	$\hat{\Delta}_4$
Representation	A_{1g}	A_{1u}	A_{2u}	E_u
Matrix form	$1, \sigma_x$	$\sigma_y s_z$	σ_z	$(\sigma_y s_x, \sigma_y s_y)$

s -wave BCS result, the ratio $\Delta(0)/T_c$ is nonuniversal and depends on the chemical potential. The obtained results can explain the observed non-BCS behavior of the superconducting order parameter $\Delta(T)$ [15, 18, 19]. Therefore, hexagonal warping may be a key for an explanation of the existence of nematic E_u superconductivity in real doped topological insulators.

II. MODEL HAMILTONIAN

We use the low-energy Hamiltonian of the bulk states of a topological insulator in the $\mathbf{k} \cdot \mathbf{p}$ model [25]. The first-order momentum expansion of this Hamiltonian is

$$H_0(\mathbf{k}) = m\sigma_x - \mu + v(k_x\sigma_z s_y - k_y\sigma_z s_x) + v_z k_z \sigma_y, \quad (1)$$

where s_i and σ_i ($i = x, y, z$) are Pauli matrices, s_i acts in the spin space, σ_i acts in the orbital space $\mathbf{p} = (P^1, P^2)$, $\mathbf{k} = (k_x, k_y)$ is the momentum, $2m$ is a single-electron gap, μ is the chemical potential, v is the Fermi velocity in the $(\Gamma K, \Gamma M)$ plane, and v_z is the Fermi velocity along the ΓZ direction.

Hamiltonian Eq. (1) is invariant under a continuous rotation in the (x, y) plane. However, the crystal structure of a real three-dimensional (3D) topological insulator (e.g., Bi_2Se_3) has only discrete threefold rotational symmetry and an anisotropic term (that is referred to as hexagonal warping), $H_w(\mathbf{k}) = \lambda(k_x^3 - 3k_x k_y^2)\sigma_z s_z$, that appears in the Hamiltonian [25]. The total single-electron Hamiltonian is $H(\mathbf{k}) = H_0(\mathbf{k}) + H_w(\mathbf{k})$. It obeys an inversion symmetry $PH(\mathbf{k})P = H(-\mathbf{k})$, where the inversion operator is $P = \sigma_x$.

We apply a U - V model to describe the electron-electron interaction. We write down the corresponding term in the Hamiltonian as $H_{\text{int}} = -U(n_1^2 + n_2^2) - 2Vn_1 n_2$ [3]. Here, $n_i = \sum_{\mathbf{k}, s} c_{i\mathbf{k}s}^\dagger c_{i\mathbf{k}s}$ and $c_{i\mathbf{k}s}^\dagger$ ($c_{i\mathbf{k}s}$) is the creation (annihilation) operator of an electron with momentum \mathbf{k} and spin projection s , and index $i = 1, 2$ corresponds to different orbitals P^i . The potentials U and V correspond to intraorbital and interorbital coupling, respectively. We consider the case of an attractive interaction, that is, $U, V > 0$. Inelastic neutron scattering measurements in $\text{Sr}_{0.1}\text{Bi}_2\text{Se}_3$ reveal that interorbital electron-phonon coupling can exceed an intraorbital one, $V > U$ [28].

III. SUPERCONDUCTING ORDER PARAMETERS

In Ref. [3] the Hamiltonian $H_0 + H_{\text{int}}$ (neglecting warping H_w) was treated using a BCS-like approach. Four possible superconducting pairing symmetries have been classified. The addition of the term H_w does not affect this classification and the results are listed in Table I.

The order parameter $\hat{\Delta}_1$ is even under inversion, while $\hat{\Delta}_2$, $\hat{\Delta}_3$, and $\hat{\Delta}_4$ are odd under this inversion. The nematic phase, that is observed in many experiments, corresponds to the vector order parameter $\hat{\Delta}_4 = (\Delta_{4x}, \Delta_{4y}) = \Delta_4(n_x, n_y)$ in E_u representation. Here, the vector $\vec{n} = (n_x, n_y) = (\cos \theta, \sin \theta)$

shows the direction of nematicity. Hexagonal warping affects the gap in the spectrum for the nematic superconductor [17]: The warping opens a full gap and this gap is the largest if $\vec{n} = (0, 1)$, and the nodes exist in the spectrum when $\vec{n} = (1, 0)$ even in the case $\lambda \neq 0$.

We use the susceptibilities χ_α to calculate the critical temperature T_c for each possible superconducting phase. The phase with the highest T_c is the ground state. Formally, we can use equations for T_c in a form presented in Ref. [3],

$$\hat{\Delta}_1 : \det \begin{pmatrix} U\chi_0(T_c) - 1 & U\chi_{01}(T_c) \\ V\chi_{01}(T_c) & V\chi_1(T_c) - 1 \end{pmatrix} = 0, \quad (2)$$

$$\hat{\Delta}_{2,4} : V\chi_{2,4}(T_c) = 1, \quad \hat{\Delta}_3 : U\chi_3(T_c) = 1,$$

where the superconducting susceptibilities ($k_B = 1$) are,

$$\chi_\alpha(T) = \int \tanh\left(\frac{\xi}{2T}\right) d\xi \int \delta(\xi_{\mathbf{k}} - \xi) \text{Tr}[(\hat{m}_\alpha P r_{\mathbf{k}})^2] d^3 \mathbf{k},$$

$$\chi_{01}(T) = \int \tanh\left(\frac{\xi}{2T}\right) d\xi \int \delta(\xi_{\mathbf{k}} - \xi) \text{Tr}[\hat{m}_0 P r_{\mathbf{k}} \hat{m}_x P r_{\mathbf{k}}] d^3 \mathbf{k}, \quad (3)$$

the integration is taken over all \mathbf{k} . Here, $\alpha = 0, 1, 2, 3, 4x, 4y$, and notation \hat{m}_α represents the matrix structure of the superconducting order parameter in the α phase that is given in Table I: $\hat{m}_0 = s_0$, $\hat{m}_1 = \sigma_x$, $\hat{m}_2 = \sigma_y s_z$, $\hat{m}_3 = \sigma_z$, $\hat{m}_{4x} = \sigma_y s_x$, $\hat{m}_{4y} = \sigma_y s_y$. The operator $\text{Tr}[\cdot \cdot \cdot]$ is the trace of a matrix and $P r_{\mathbf{k}} = \sum_{j=1,2} |\phi_{j,\mathbf{k}}\rangle \langle \phi_{j,\mathbf{k}}|$, $\phi_{j,\mathbf{k}}$ is an eigenvector of the Hamiltonian, and $\xi_{\mathbf{k}}$ is the quasiparticle spectrum in the normal state, $(H_0 + H_w)\phi_{j,\mathbf{k}} = \xi_{\mathbf{k}}\phi_{j,\mathbf{k}}$. Since k_z enters into integrands only with a factor v_z , integrals (3) are proportional to $1/v_z$ and the phase diagram does not depend on v_z .

We also compute the system free energy at $T = 0$ for different order parameter symmetries to verify the results obtained with the help of the superconducting susceptibilities. The phase diagrams near $T = T_c$ and $T = 0$ are the same. Note that values of the order parameters of competing phases are finite at the boundaries of the phase diagram.

IV. PHASE DIAGRAM

A numerical analysis of Eqs. (2) and (3) with Hamiltonian $H_0 + H_w + H_{\text{int}}$ shows that the phase $\hat{\Delta}_3$ always has lower T_c than $\hat{\Delta}_1$. Depending on the parameters, the ground state of the system can be $\hat{\Delta}_1$, $\hat{\Delta}_2$, or $\hat{\Delta}_4$. In contrast, in the case $\lambda = 0$ only $\hat{\Delta}_1$ and $\hat{\Delta}_2$ are candidates for this role [3].

In the nematic phase $\hat{\Delta}_4$, the calculated order parameter and T_c are the same for any direction of nematicity \vec{n} . When $\lambda \neq 0$, a full gap in the spectrum opens in the case Δ_{4y} and the free energy is the smallest for this direction of nematicity. Note that the difference in the free energy between Δ_{4y} and Δ_{4x} is much smaller than the typical difference between the free energies of other phases away from the phase boundaries. It means, in particular, that a small strain can change the relation between the Δ_{4y} and Δ_{4x} states. We also analyze the possible existence of a chiral phase with the order parameter $\Delta_{4y} \pm i\Delta_{4x}$, which spontaneously breaks the time-reversal symmetry. This phase has the same T_c as Δ_{4y} but a higher free energy. However, the chiral phase could be favorable for an extremely small ratio of $v_z/v \ll 1$ and

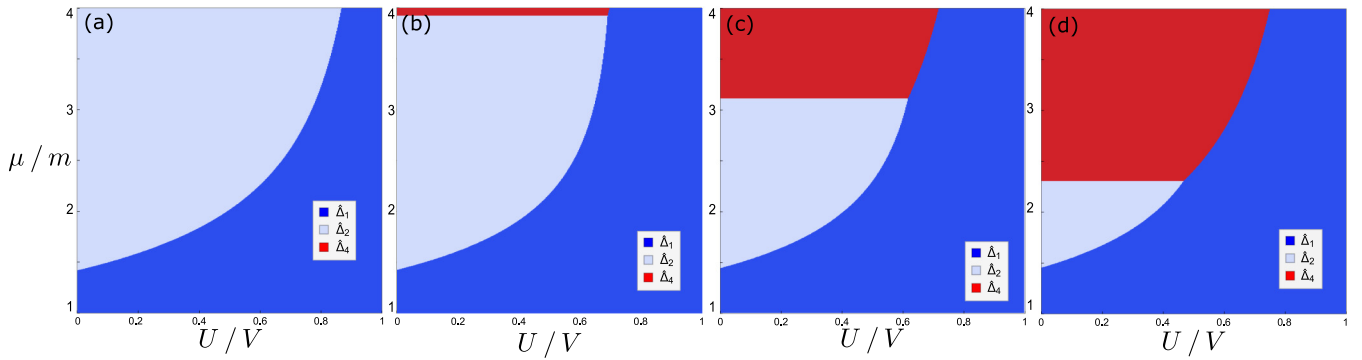


FIG. 1. The phase diagram in the plane $(U/V, \mu/m)$. The blue area corresponds to the ground state with the order parameter $\hat{\Delta}_1$ (or A_{1g}), the gray area corresponds to $\hat{\Delta}_2$ (A_{2g}), and the red area corresponds to the nematic order parameter $\hat{\Delta}_4$ (E_u). (a)–(d) show phase diagrams for different values of the hexagonal warping, $\lambda m^2/v^3 = 0, 0.3, 0.5$, and 1 , respectively.

large warping. A similar result was obtained in Ref. [29] for the model Hamiltonian with a different type of spectrum nonlinearity.

We introduce the following dimensionless parameters: the chemical potential μ/m , hexagonal warping $\lambda m^2/v^3$, and interaction U/V . The computed phase diagram of the system is shown in Fig. 1 in the plane $(U/V, \mu/m)$ for different $\lambda m^2/v^3$. The singlet pairing $\hat{\Delta}_1$ is the only ground state if $U > V$. The phase diagram becomes reachable when $V > U$. In the absence of warping, the ground state is either $\hat{\Delta}_1$ or $\hat{\Delta}_2$ depending on the chemical potential [Fig. 1(a)]. In the case of small warping [Fig. 1(b)], the nematic phase $\hat{\Delta}_4$ becomes a ground state at a large chemical potential and the area with a stable nematic E_u pairing rapidly increases with an increase of $\lambda m^2/v^3$ [Figs. 1(c) and 1(d)].

The phase diagram in the plane $(\lambda m^2/v^3, \mu/m)$ is shown in Fig. 2 for different values U/V . As we can see, a moderate ratio between interorbital V and intraorbital U couplings is favorable for nematic ordering. The increase of the chemical potential benefits both $\hat{\Delta}_2$ and nematic $\hat{\Delta}_4$ pairings. The increase of hexagonal warping makes the $\hat{\Delta}_2$ phase less favorable in comparison to both $\hat{\Delta}_1$ and nematic pairings. The growth of μ/m stimulates the nematic phase Δ_{4y} , as compared

to the pairing $\hat{\Delta}_1$, especially at small values of the intraorbital interaction U .

The nematic pairing $\hat{\Delta}_4 : (c_{k1\uparrow}c_{-k2\uparrow} + c_{k1\downarrow}c_{-k2\downarrow})$ [17] couples electrons in different orbitals with the same spin. If we neglect the hexagonal warping, the numbers of electrons with opposite spin projection are equal at each orbital. The hexagonal warping $H_w = \lambda(k)s_z\sigma_z$ shifts this spin projection balance: The moving electrons obeying a given orbital become polarized, while the total polarization of the electron liquid remains zero. Thus, hexagonal warping favors nematic superconductivity since it creates a favorable spin-orbit configuration.

V. MEAN-FIELD CALCULATIONS FOR E_u PAIRING

Here, we calculate the absolute value Δ of the nematic order parameter $\hat{\Delta}_4 = \Delta(0, 1)$. We choose the Nambu basis as $\Psi_{\mathbf{k}} = (\phi_{\mathbf{k}}, -i s_y \phi_{-\mathbf{k}}^\dagger)^t$, where $\phi_{\mathbf{k}} = (\phi_{\uparrow,1,\mathbf{k}}, \phi_{\downarrow,1,\mathbf{k}}, \phi_{\uparrow,-1,\mathbf{k}}, \phi_{\downarrow,-1,\mathbf{k}})^t$ and the superscript t means transposition. In this basis the mean-field Hamiltonian of the topological insulator with a nematic superconducting

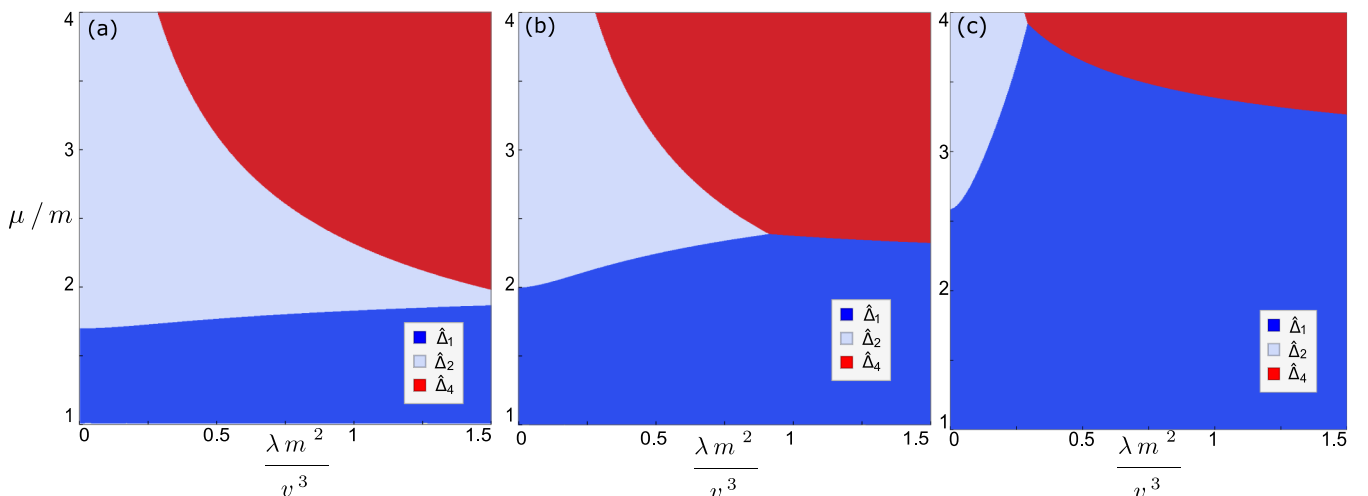


FIG. 2. The phase diagram in the plane $(\lambda m^2/v^3, \mu/m)$ for different values of the interaction parameter U/V . The notations for the ground state are the same as in Fig. 1. (a)–(c) show the phase diagrams at $U/V = 0.3, 0.5$, and 0.7 , respectively.

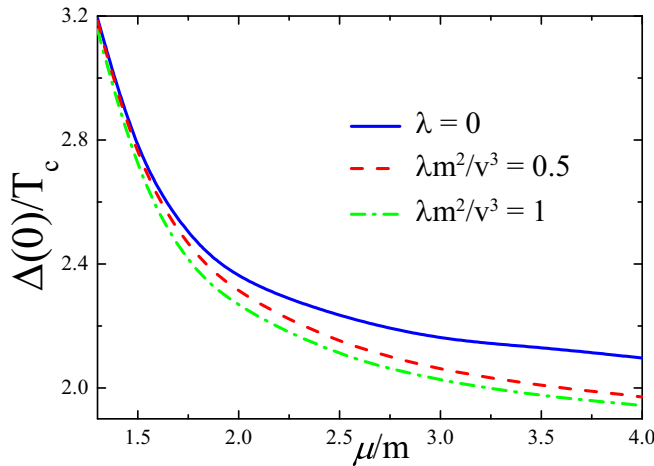


FIG. 3. Ratio of the order parameter at zero temperature and the critical temperature, $\Delta(0)/T_c$, as a function of the chemical potential for different values of the hexagonal warping. The blue line corresponds to $\lambda = 0$, the red dashed line to $\lambda m^2/v^3 = 0.5$, and the green dotted-dashed line to $\lambda m^2/v^3 = 1$.

order can be written as

$$H_{\text{BdG}}(\mathbf{k}) = (H_0 + H_w)\tau_z + \Delta\sigma_y s_y \tau_x, \quad (4)$$

where τ_i is the Pauli matrix in the electron-hole space. Keeping in mind that in terms of the creation-annihilation operators the nematic order corresponds to $c_{1\sigma}c_{2\sigma}$ pairing [3], we can write the mean-field free energy in the form

$$\Omega = \frac{2\Delta^2}{V} - 2T \sum_i \int \frac{d^3k}{(2\pi)^3} \ln \left\{ 1 + \exp \left[-\frac{\epsilon_i(\mathbf{k})}{T} \right] \right\}, \quad (5)$$

where $\epsilon_i(\mathbf{k})$ is the i th eigenvalue of H_{BdG} . We compute $\Delta(T)$ by minimizing Ω . These calculations reveal that the ratio $\Delta(0)/T_c$ is not a constant in contrast to the s -wave BCS superconductivity and depends on the chemical potential and the warping (see Fig. 3). The value $\Delta(0)/T_c$ decreases with μ and λ and may be considerably larger than the BCS value 1.76. In Fig. 4 we show that the dependence of $\Delta(T)/\Delta(0)$ on temperature can be approximated as $\Delta(T)/\Delta(0) \approx \sqrt{1 - (T/T_c)^3}$ for the entire range of temperatures and is almost independent of the value of hexagonal warping. In Ref. [19] the dependence of the gap in $\text{Nb}_x\text{Bi}_2\text{Se}_3$ on temperature has been measured. The results are shown in Fig. 4 by pink triangles. As we can see from this figure, the theory fits the experiment well.

VI. DISCUSSION

We show that the existence of hexagonal warping can explain the experimental observations of E_u superconducting pairing in doped topological insulators if the dimensionless parameters $\lambda m^2/v^3$ and μ/m are not small. In undoped Bi_2Se_3 , the chemical potential lies near the band edge $\mu/m = 1.3$ and the strength of the warping is estimated as $\lambda m^2/v^3 = 0.11$ [25]. These values are too small for the existence of a nematic phase. However, the doping by Cu or Sb can significantly increase the chemical potential and the value $\mu/m = 2$ or larger looks realistic [30,31]. The Fermi velocity

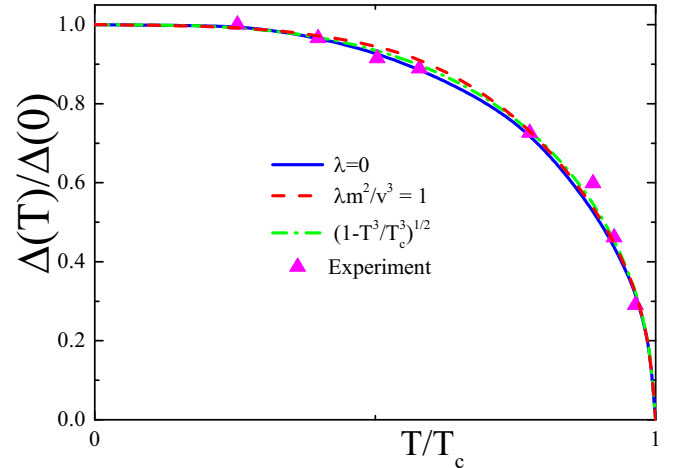


FIG. 4. Dependence of the order parameter Δ on temperature for different values of hexagonal warping. The blue line corresponds to zero warping, the red line to $\lambda m^2/v^3 = 1$, and both curves are plotted at $\mu/m = 2$. The green dotted-dashed line is a fit $\Delta(T)/\Delta(0) = \sqrt{1 - (T/T_c)^3}$. Purple triangles correspond to the experimental data extracted from Ref. [19].

also significantly affects the warping parameter $\lambda m^2/v^3$. The reported Fermi velocities for the surface states in the topological insulators lie in a wide range from $v = 5 \times 10^7$ cm/s in Ref. [32] to $v = 10^7$ cm/s in Ref. [33] and even down to $v = 3 \times 10^5$ cm/s in Ref. [34]. Thus, the necessary large value of the effective hexagonal warping is realistic. For example, if the Fermi velocity for the bulk states v decreases by half in comparison with density functional theory (DFT) calculations for undoped Bi_2Se_3 , then the warping parameter increases by eight, $\lambda m^2/v^3 \approx 0.9$, and the nematic phase become favorable. It is hard to estimate the ratio of the intraorbital to interorbital attraction U/V . In Ref. [21] the electron-phonon couplings have been calculated for $\text{Cu}_{0.16}\text{Bi}_2\text{Se}_3$ using the DFT approach under an assumption of a weak effect of Cu doping on the structural properties. It has been obtained that the triplet pairing A_{2g} has a lower free energy than A_{1g} . In our terms, it means that $V > U$, which is necessary for nematic E_u pairing. However, the x-ray experiments show that even small doping has a considerable effect on the structural properties of topological insulators [16,35], so the values v and λ can be also affected by doping.

The gap in the energy spectrum $2\bar{\Delta}$ relates to the order parameter as $\bar{\Delta} = \Delta \lambda k_F^2/\mu$ when $\Delta \ll v/k_F$, where k_F is the Fermi momentum in the normal state in the ΓK direction. In Ref. [15] the superconducting gap in $\text{Cu}_x\text{Bi}_2\text{Se}_3$ was estimated as $\bar{\Delta} \approx 0.256$ meV in a sample with $T_c \sim 3$ K. If we take typical values for the nematic superconductivity $\lambda m^2/v^3 = 0.5$ and $\mu/m = 3$ (see Fig. 2), then we get $\bar{\Delta} \approx 0.35\Delta$. Using these parameters we get an estimate $\Delta(0)/T_c \approx 2.4$ for the $\text{Cu}_x\text{Bi}_2\text{Se}_3$ samples, which is in good agreement with the result shown in Fig. 3.

The Anderson theorem is valid in the case of the considered topological superconductivity [36], and weak disorder does not affect significantly the obtained results. The influence of fluctuations on nematic superconductivity has been studied in Ref. [4] using a simplified parabolic Hamiltonian. The fluctuations generate attraction in both the s -wave and nematic

channels, while the fluctuations in the A_{1u} and A_{2u} channels stimulate the s -wave pairing. Thus, we expect that fluctuations increase the region of the nematic and s -wave phases in the phase diagram.

VII. CONCLUSION

We suggest a possible mechanism of the ground-state nematic superconductivity with the spin-triplet E_u pairing which is observed in doped topological insulators. We show that hexagonal warping is an essential feature for the realization of nematic superconductivity. Nematic superconductivity has a non-BCS behavior of the order parameter. In particular, the

ratio of the order parameter at $T = 0$ to the critical temperature is nonuniversal and depends on the chemical potential and warping.

ACKNOWLEDGMENTS

A.L.R. acknowledges the support by JSPS-RFBR Grant No. 19-52-50015 and RFBR Grant No. 19-02-00421. R.S.A. and D.A.K. were supported by the Russian Scientific Foundation under Grant No. 20-72-00030 and the Foundation for the Advancement of Theoretical Physics and Mathematics BASIS.

-
- [1] X.-L. Qi and S.-C. Zhang, Topological insulators and superconductors, *Rev. Mod. Phys.* **83**, 1057 (2011).
- [2] L. Fu and C. L. Kane, Superconducting Proximity Effect and Majorana Fermions at the Surface of a Topological Insulator, *Phys. Rev. Lett.* **100**, 096407 (2008).
- [3] L. Fu and E. Berg, Odd-Parity Topological Superconductors: Theory and Application to $\text{Cu}_x\text{Bi}_2\text{Se}_3$, *Phys. Rev. Lett.* **105**, 097001 (2010).
- [4] F. Wu and I. Martin, Nematic and chiral superconductivity induced by odd-parity fluctuations, *Phys. Rev. B* **96**, 144504 (2017).
- [5] L. Hao and C. S. Ting, Nematic superconductivity in $\text{Cu}_x\text{Bi}_2\text{Se}_3$: Surface Andreev bound states, *Phys. Rev. B* **96**, 144512 (2017).
- [6] M. Hecker and J. Schmalian, Vestigial nematic order and superconductivity in the doped topological insulator $\text{Cu}_x\text{Bi}_2\text{Se}_3$, *npj Quantum Mater.* **3**, 26 (2018).
- [7] H. Uematsu, T. Mizushima, A. Tsuruta, S. Fujimoto, and J. A. Sauls, Chiral Higgs Mode in Nematic Superconductors, *Phys. Rev. Lett.* **123**, 237001 (2019).
- [8] H. Huang, J. Gu, P. Ji, Q. Wang, X. Hu, Y. Qin, J. Wang, and C. Zhang, Giant anisotropic magnetoresistance and planar Hall effect in $\text{Sr}_{0.06}\text{Bi}_2\text{Se}_3$, *Appl. Phys. Lett.* **113**, 222601 (2018).
- [9] T. Kawai, C. G. Wang, Y. Kandori, Y. Honoki, K. Matano, T. Kambe, and G.-q. Zheng, Direction and symmetry transition of the vector order parameter in topological superconductors $\text{Cu}_x\text{Bi}_2\text{Se}_3$, *Nat. Commun.* **11**, 235 (2020).
- [10] S. Yonezawa, Nematic superconductivity in doped Bi_2Se_3 topological superconductors, *Condens. Matter* **4**, 2 (2018).
- [11] K. Matano, M. Kriener, K. Segawa, Y. Ando, and G.-q. Zheng, Spin-rotation symmetry breaking in the superconducting state of $\text{Cu}_x\text{Bi}_2\text{Se}_3$, *Nat. Phys.* **12**, 852 (2016).
- [12] S. Yonezawa, K. Tajiri, S. Nakata, Y. Nagai, Z. Wang, K. Segawa, Y. Ando, and Y. Maeno, Thermodynamic evidence for nematic superconductivity in $\text{Cu}_x\text{Bi}_2\text{Se}_3$, *Nat. Phys.* **13**, 123 (2016).
- [13] Y. Pan, A. M. Nikitin, G. K. Araizi, Y. K. Huang, Y. Matsushita, T. Naka, and A. de Visser, Rotational symmetry breaking in the topological superconductor $\text{Sr}_x\text{Bi}_2\text{Se}_3$ probed by upper-critical field experiments, *Sci. Rep.* **6**, 28632 (2016).
- [14] M. Chen, X. Chen, H. Yang, Z. Du, and H.-H. Wen, Superconductivity with twofold symmetry in $\text{Bi}_2\text{Te}_3/\text{FeTe}_{0.55}\text{Se}_{0.45}$ heterostructures, *Sci. Adv.* **4**, eaat1084 (2018).
- [15] R. Tao, Y.-J. Yan, X. Liu, Z.-W. Wang, Y. Ando, Q.-H. Wang, T. Zhang, and D.-L. Feng, Direct Visualization of the Nematic Superconductivity in $\text{Cu}_x\text{Bi}_2\text{Se}_3$, *Phys. Rev. X* **8**, 041024 (2018).
- [16] A. Y. Kuntsevich, M. A. Bryzgalov, R. S. Akzyanov, V. P. Martovitskii, A. L. Rakhmanov, and Y. G. Selivanov, Strain-driven nematicity of odd-parity superconductivity in $\text{Sr}_x\text{Bi}_2\text{Se}_3$, *Phys. Rev. B* **100**, 224509 (2019).
- [17] L. Fu, Odd-parity topological superconductor with nematic order: Application to $\text{Cu}_x\text{Bi}_2\text{Se}_3$, *Phys. Rev. B* **90**, 100509(R) (2014).
- [18] T. Kirzhner, E. Lahoud, K. B. Chaska, Z. Salman, and A. Kanigel, Point-contact spectroscopy of $\text{Cu}_{0.2}\text{Bi}_2\text{Se}_3$ single crystals, *Phys. Rev. B* **86**, 064517 (2012).
- [19] A. Sirohi, S. Das, P. Neha, K. S. Jat, S. Patnaik, and G. Sheet, Low-energy excitations and non-BCS superconductivity in $\text{Nb}_x\text{-Bi}_2\text{Se}_3$, *Phys. Rev. B* **98**, 094523 (2018).
- [20] P. M. R. Brydon, S. Das Sarma, H.-Y. Hui, and J. D. Sau, Odd-parity superconductivity from phonon-mediated pairing: Application to $\text{Cu}_x\text{Bi}_2\text{Se}_3$, *Phys. Rev. B* **90**, 184512 (2014).
- [21] X. Wan and S. Y. Savrasov, Turning a band insulator into an exotic superconductor, *Nat. Commun.* **5**, 4144 (2014).
- [22] V. Kozii and L. Fu, Odd-Parity Superconductivity in the Vicinity of Inversion Symmetry Breaking in Spin-Orbit-Coupled Systems, *Phys. Rev. Lett.* **115**, 207002 (2015).
- [23] C. Chen, Z. Xie, Y. Feng, H. Yi, A. Liang, S. He, D. Mou, J. He, Y. Peng, X. Liu, Y. Liu, L. Zhao, G. Liu, X. Dong, J. Zhang, L. Yu, X. Wang, Q. Peng, Z. Wang, S. Zhang, F. Yang, C. Chen, Z. Xu, and X. J. Zhou, Tunable Dirac fermion dynamics in topological insulators, *Sci. Rep.* **3**, 2411 (2013).
- [24] L. Fu, Hexagonal Warping Effects in the Surface States of the Topological Insulator Bi_2Te_3 , *Phys. Rev. Lett.* **103**, 266801 (2009).
- [25] C.-X. Liu, X.-L. Qi, H. J. Zhang, X. Dai, Z. Fang, and S.-C. Zhang, Model Hamiltonian for topological insulators, *Phys. Rev. B* **82**, 045122 (2010).
- [26] R. S. Akzyanov and A. L. Rakhmanov, Surface charge conductivity of a topological insulator in a magnetic field: The effect of hexagonal warping, *Phys. Rev. B* **97**, 075421 (2018).
- [27] R. S. Akzyanov and A. L. Rakhmanov, Bulk and surface spin conductivity in topological insulators with hexagonal warping, *Phys. Rev. B* **99**, 045436 (2019).
- [28] J. Wang, K. Ran, S. Li, Z. Ma, S. Bao, Z. Cai, Y. Zhang, K. Nakajima, S. Ohira-Kawamura, P. Čermák, A. Schneidewind,

- S. Y. Savrasov, X. Wan, and J. Wen, Evidence for singular-phonon-induced nematic superconductivity in a topological superconductor candidate $\text{Sr}_{0.1}\text{Bi}_2\text{Se}_3$, *Nat. Commun.* **10**, 2802 (2019).
- [29] L. Chirolli, Chiral superconductivity in thin films of doped Bi_2Se_3 , *Phys. Rev. B* **98**, 014505 (2018).
- [30] E. Lahoud, E. Maniv, M. S. Petrushevsky, M. Naamneh, A. Ribak, S. Wiedmann, L. Petaccia, Z. Salman, K. B. Chashka, Y. Dagan, and A. Kanigel, Evolution of the Fermi surface of a doped topological insulator with carrier concentration, *Phys. Rev. B* **88**, 195107 (2013).
- [31] M. Neupane, Y. Ishida, R. Sankar, J.-X. Zhu, D. S. Sanchez, I. Belopolski, S.-Y. Xu, N. Alidoust, M. M. Hosen, S. Shin, F. Chou, M. Z. Hasan, and T. Durakiewicz, Electronic structure and relaxation dynamics in a superconducting topological material, *Sci. Rep.* **6**, 22557 (2016).
- [32] H. Zhang, C.-X. Liu, X.-L. Qi, X. Dai, Z. Fang, and S.-C. Zhang, Topological insulators in Bi_2Se_3 , Bi_2Te_3 and Sb_2Te_3 with a single Dirac cone on the surface, *Nat. Phys.* **5**, 438 (2009).
- [33] M. Veldhorst, M. Snelder, M. Hoek, T. Gang, V. K. Guduru, X. L. Wang, U. Zeitler, W. G. van der Wiel, A. A. Golubov, H. Hilgenkamp, and A. Brinkman, Josephson supercurrent through a topological insulator surface state, *Nat. Mater.* **11**, 417 (2012).
- [34] A. Wolos, S. Szyszko, A. Drabinska, M. Kaminska, S. G. Strzelecka, A. Hruban, A. Materna, and M. Piersa, Landau-Level Spectroscopy of Relativistic Fermions with Low Fermi Velocity in the Bi_2Te_3 Three-Dimensional Topological Insulator, *Phys. Rev. Lett.* **109**, 247604 (2012).
- [35] A. Y. Kuntsevich, M. A. Bryzgalov, V. A. Prudkoglyad, V. P. Martovitskii, Y. G. Selivanov, and E. G. Chizhevskii, Structural distortion behind the nematic superconductivity in $\text{Sr}_x\text{Bi}_2\text{Se}_3$, *New J. Phys.* **20**, 103022 (2018).
- [36] L. Andersen, A. Ramires, Z. Wang, T. Lorenz, and Y. Ando, Generalized Anderson's theorem for superconductors derived from topological insulators, *Sci. Adv.* **6**, eaay6502 (2020).